Proceedings of IMECE2005
2005 ASME International Mechanical Engineering Congress and Exposition
November 5-11, 2005, Orlando, Florida USA

IMECE2005-80129

ARCHITECTURE AND HYDRAULICS OF A LOWER EXTREMITY EXOSKELETON

Adam Zoss, H. Kazerooni
Department of Mechanical Engineering
University of California, Berkeley, CA, 94720, USA
exo@berkeley.edu, http://bleex.me.berkeley.edu

ABSTRACT

Wheeled vehicles are often incapable of transporting heavy materials over rough terrain or up staircases. Lower extremity exoskeletons supplement human intelligence with the strength and endurance of a pair of wearable robotic legs that support a payload. This paper summarizes the design and analysis of the Berkeley Lower Extremity Exoskeleton (BLEEX). The anthropomorphically-based BLEEX has seven degrees of freedom per leg, four of which are powered by linear hydraulic actuators. The selection of the degrees of freedom, critical hardware design aspects, and initial performance measurements of BLEEX are discussed.

INTRODUCTION

Heavy objects are typically transported by wheeled vehicles. However, many environments, such as rocky slopes and staircases, pose significant challenges to wheeled vehicles. Within these settings, legged locomotion becomes an attractive method of transportation, since legs can adapt to a wide range of extreme terrains. Berkeley's lower extremity exoskeleton (BLEEX) is the first field-operational robotic system which is worn by its operator and provides the ability to carry significant loads with minimal effort over any type of terrain.

BLEEX is comprised of two powered anthropomorphic legs, a power supply, and a backpack-like frame on which a variety of heavy payloads can be mounted. BLEEX provides load carrying capability through legged locomotion guided by human interaction, but instead of actively "driving" the vehicle, BLEEX shadows the operator's movement as he/she "wears" it like a pair of artificial legs. By combining the strength capabilities of robotics with the navigational intelligence and adaptability of humans, BLEEX allows heavy loads to be carried over rough, unstructured, and uncertain terrains. Possible applications include helping soldiers, disaster relief workers, wildfire fighters, and other emergency personnel to carry major loads without the strain typically associated with demanding labor.

BACKGROUND

In the late 1960's, the first active exoskeletons were developed almost simultaneously at General Electric (GE) [1] and the Mihajlo Pupin Institute in Belgrade [2]. Safety concerns and complexity prevented the Hardiman project at GE from walking and the Belgrade exoskeleton only followed pre-programmed walking motions. Both projects were tethered to a stationary power source.

More recently Tsukuba University developed a lightweight power assist device, HAL [3]. It successfully walks and carries its own power supply, but it is designed to only assist the wearer's muscles; it cannot carry an external load. The Kanagawa Institute of Technology created a full-body "wearable power suit", powered by unique pneumatic actuators [4]. It has been demonstrated in limited applications without a portable power supply.

Still in development are several other lower extremity exoskeletons designed to aid disabled people ([5]–[7]). Similar to exoskeletons, a variety of orthoses are being developed for the knee [8]-[9], lower back [10], and ankle [11].

The BLEEX project is an energetically autonomous exoskeleton capable of carrying its own weight plus an external payload. All previous exoskeletons are either tethered to a fixed power supply or not strong enough to carry an external load. Unlike orthoses and braces, BLEEX transfers the payload forces to the ground, instead of the wearer.

EXOSKELETON CONTROL

The BLEEX control algorithm ensures that the exoskeleton shadows the operator with minimal interaction forces between the two. The highlight of the control scheme is that it is solely based on measurements from the exoskeleton; there are no direct measurements from the operator or from where the operator contacts the exoskeleton (e.g. no force sensors between the two) [12]. This eliminates the problems associated with measuring interaction forces or human muscle activity.

Through the control algorithm, BLEEX instantaneously shadows the wearer's voluntary and involuntary movements. This requires the controller to be very sensitive to all forces and torques the operator imposes on the exoskeleton. To achieve this, the BLEEX control increases the closed loop system sensitivity to the operator's forces and torques [12].

The BLEEX control scheme uses a full dynamic model of the exoskeleton and utilizes a significant number of sensors to solve the dynamic model and control its actuators; thus BLEEX contains a large amount of electronics. Each actuated joint contains an encoder and a pair of linear accelerometers to determine the joint's angle, angular velocity, and angular acceleration. An inclinometer gives the overall orientation relative to gravity. Servo valves and single axis force sensors provide control and feedback of the actuation forces. Foot switches determine when the exoskeleton feet touch the ground and load distribution sensors determine how the operator distributes their own weight between their two feet in double stance. All the sensors connect to a distributed network of electronic boards (remote I/O modules or RIOMs), which then connect to a centralized controlling computer [13]. Table 1 summarizes the amount of electronics required for the BLEEX control algorithm.

Electronics	Qty. per Actuator	Qty. per Exoskeleton
Encoder	1	8
Linear Accelerometer	2	16
Single Axis Force Sensor	1	8
Servo Valve	1	8
RIOMs	1	10
Foot Switches	N/A	2
Load Distribution Sensor	N/A	2
Inclinometer	N/A	1
Control Computer	N/A	1

Table 1: BLEEX Electronic Requirements

DEGREES OF FREEDOM

To ensure maximum safety and minimum collisions with the environment and operator, the BLEEX architecture is almost anthropomorphic. This means the BLEEX leg is kinematically similar to a human's, but does not include all of the degrees of freedom (DoF) of human legs. Additionally, the BLEEX degrees of freedom are all purely rotary joints. While the details of these joints differ from human joints, BLEEX has hip, knee, and ankle joints, like a person. Overall, BLEEX has seven distinct degrees of freedom per leg:

- 3 DoF at the hip
- 1 DoF at the knee (pure rotation in the sagittal plane)
- 3 DoF at the ankle

Additionally, the front of the exoskeleton foot, under the operator's toes, is compliant to allow the exoskeleton foot to flex with the human's foot (see "Foot Design" Section).

Since the human and exoskeleton leg kinematics are not exactly the same (merely similar), the human and exoskeleton are only rigidly connected at the extremities (feet and torso).

RANGE OF MOTION

The BLEEX kinematics are close to human leg kinematics, so the BLEEX joint ranges of motion are determined by examining human joint ranges of motion. At the very least, the BLEEX joint range of motion should be equal to the human range of motion during walking (shown in column 1 in Table 2), which can be found by examining Clinical Gait Analysis (CGA) data ([14]–[16]). Safety dictates that the BLEEX range of motion should not be more than the operator's range of motion (shown in Column 3 of Table 2) [17]. For each degree of freedom, the second column of Table 2 lists the BLEEX range of motion which is, in general, larger than the human range of motion during walking and less than the maximum range of human motion.

	Human Walking Maximum	BLEEX Maximum	Average Military Male Maximum
Ankle Flexion	14.1°	45°	35°
Ankle Extension	20.6°	45°	38°
Ankle Abduction	not available	20°	23°
Ankle Adduction	not available	20°	24°
Knee Flexion	73.5°	121°	159°
Hip Flexion	32.2°	121°	125°
Hip Extension	22.5°	10°	not available
Hip Abduction	7.9°	16°	53°
Hip Adduction	6.4°	16°	31°
Total Rotation External	13.2°	35°	73°
Total Rotation Internal	1.6°	35°	66°

Table 2: BLEEX Joint Ranges of Motion

The most maneuverable exoskeleton should ideally have ranges of motion slightly less than the human's maximum range of motion. However, BLEEX uses linear actuators (see "Actuator Selection and Sizing" section), so some of the joint ranges of motion are reduced to prevent the actuators' axes of motion from passing through the joint center. If this had not been prevented, the joint could reach a configuration where the actuator would be unable to produce a torque about its joint. Additionally, all the joint ranges of motion were tested and revised during prototype testing. For example, mock-up testing determined that the BLEEX ankle flexion/extension range of motion needs to be greater than the human ankle range of motion to accommodate the human foot's smaller degrees of freedom not modeled in the BLEEX foot.

WHICH JOINTS TO ACTUATE?

Each BLEEX leg has 7 DoF (besides the toe flexibility), but actuating them all creates unnecessarily high power consumption and control complexity. Instead, only joints that require substantial power should be actuated. As a first step, the actuation was designed primarily for walking, so CGA data was used to determine which degrees of freedom consume power while walking. This also assumes the BLEEX leg masses and inertias are similar to a human leg.

The flexion/extension DoF at the ankle, knee, and hip see the highest amount of power ([18], [19], Fig. 1). The ankle and hip both consume power (positive power) and thus need to be actuated. The knee mainly absorbs power (negative power) while walking; however, when climbing steps or squatting the knee becomes critical for adding power to the system [20] (Fig. 2). Therefore, the knee joint is also actuated.

Besides flexion/extension joints, hip abduction/adduction requires the most power during walking as it provides the lateral balancing forces; thus, the BLEEX hip abduction/ adduction joints are actuated. According to CGA data, the

other degrees of freedom (hip rotation, ankle rotation, and ankle abduction/adduction) have very small power consumptions while walking, so they remain un-actuated (Fig. 1). The un-actuated joints still may have springs, or other impedances, to reduce the load on human muscles and increase comfort.

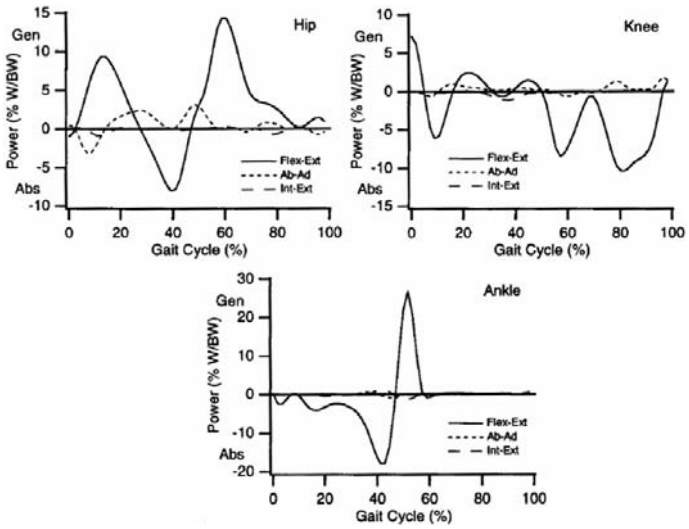

Fig. 1: Human Power Required for Walking. The most power is required by the flexion/extension joints in the ankle, knee, and hip. The hip abduction/adduction requires the next most power. [18]

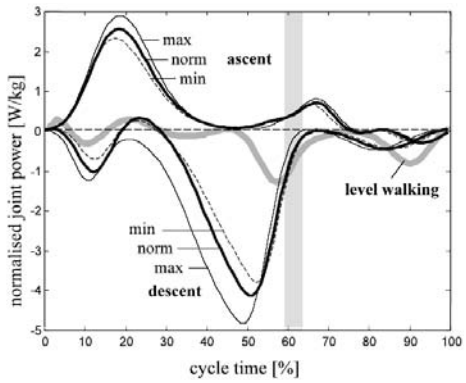

Fig. 2: Knee Power Required for Ascending/Descending Stairs. The knee requires significant power when ascending stairs (instead of absorbing power like it does during level walking) [20].

ACTUATOR SELECTION AND SIZING

Hydraulic actuators have high specific power (ratio of actuator power to actuator weight), and thus are the smallest actuation option available. Also, hydraulic fluid is generally incompressible, leading to a relatively high control bandwidth. BLEEX uses double-acting linear hydraulic actuators because of their compact size, low weight, and high force capabilities. Rotary hydraulic actuators were not selected because they usually have either internal leakage or considerable friction.

In order to analytically determine the appropriate size of actuators, an equation for the actuator's torque capabilities must be determined. The maximum static pushing and pulling forces that a linear hydraulic actuator cylinder can supply is its cross-sectional area multiplied by the supply pressure (P_S). When a linear actuator is used to produce a torque about a rotary joint, its moment arm, R, changes as a function of the joint angle, θ (Fig. 3). The torque the actuator can produce is its peak force times that moment arm:

$$T_{\max\ push} = P_S \cdot \frac{\pi D_{bore}^2}{4} \cdot R(\theta) \quad (1)$$

$$T_{\max\ pill} = P_S \cdot \frac{\pi\left(D_{bore}^2 - D_{rod}^2\right)}{4} \cdot R(\theta) \quad (2)$$

where D_{bore} is the actuator bore diameter and D_{rod} is the actuator rod diameter.

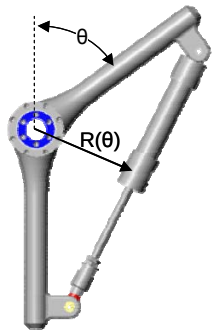

Fig. 3: Triangular Configuration of a Linear Actuator about a Rotary Joint. The moment arm, R, is perpendicular to the actuator and varies with joint angle θ.

The problem of actuation design is to find a combination of actuator cross-section, actuator endpoints, and supply pressure that provides the necessary torque, but minimizes the hydraulic consumption. Since the BLEEX dynamics are close to human leg dynamics, the actuators must produce torque greater than the CGA data in order to walk. Additionally, the actuator must reach the desired ranges of motion while always being able to produce a minimum nominal torque. In general, there is not a unique solution, but many feasible possibilities.

To find a feasible actuator configuration, an actuator size (cross-section, minimum length, and stroke), supply pressure, and one of the end-point positions were chosen for each joint. Assuming that the longest and shortest actuator lengths occur at the extremes of the joint's range of motion, the second end-point position of the actuator can be calculated (Fig. 4). Then the available actuator torque (Eq. 1 and Eq. 2) can be compared with the required torques (as determined from CGA data). This process was iterated for each joint with different actuator sizes, mounting points, or supply pressures until a solution with sufficient torque and minimal power consumption was found.

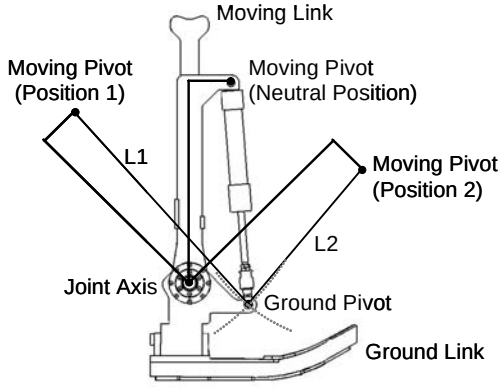

Fig. 4: Solving for the Actuator End-Point. First, an actuator and moving pivot location (in the neutral position) were chosen. The actuator is fully extended (length L1) and fully contracted (length L2) at the limits of motion (positions 1 & 2). The second end-point, the ground pivot, is found by the intersection of arcs of radii L1 and L2 centered at the moving pivot positions 1 & 2.

Fig. 5 – Fig. 7 show the maximum torque vs. angle plots (from Eq. 1 and Eq. 2) for the BLEEX actuation compared to CGA data for the ankle, knee, and hip. BLEEX utilizes the smallest commercially available actuators (about 2 cm bore) along with a relatively low supply pressure of 6.9 MPa. The sign conventions for the joint angles and torques are illustrated in Fig. 8.

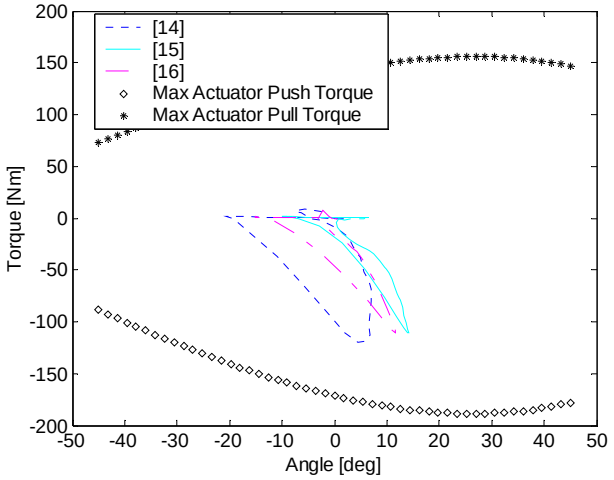

Fig. 5: Ankle Torque vs. Angle for CGA Data and the Max Actuator Torque

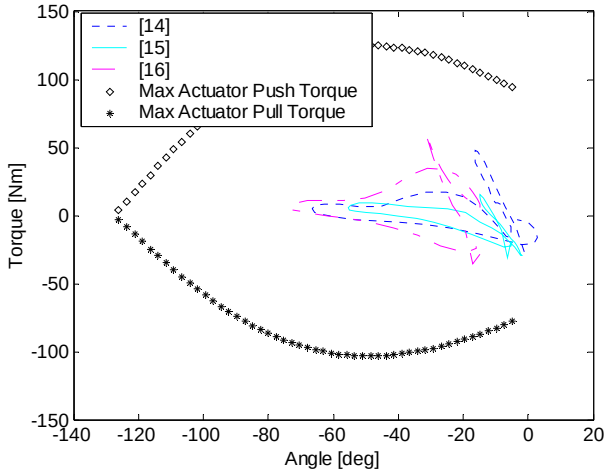

Fig. 6: Knee Torque vs. Angle for CGA Data and the Max Actuator Torque

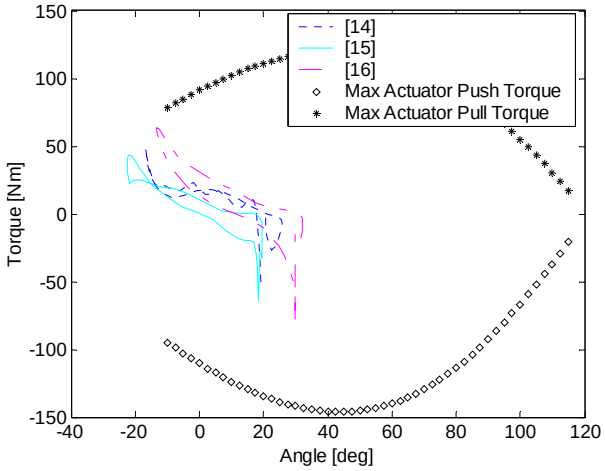

Fig. 7: Hip Torque vs. Angle for CGA Data and the Max Actuator Torque

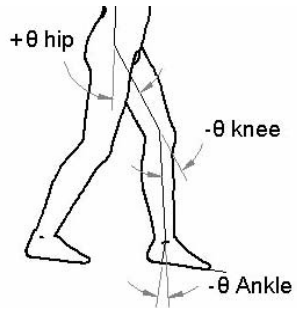

Fig. 8: Angle and Torque Sign Conventions. Each joint angle is measured as the positive counterclockwise displacement of the distal link from the proximal link (zero in the standing position).

VALVE SELECTION

Once the actuator size and end-points were selected, servo valves were chosen that are as small as possible, but still provide the necessary hydraulic flow rates. Similar to the actuator selection, CGA data was used to select the appropriate sized valves for BLEEX. The actuator hydraulic flow rate, Q_{push} and Q_{pull}, and pressure, P_{push} and P_{pull}, required to provide the CGA torques and angular velocities are calculated based on the actuator geometry:

$$Q_{push} = R(\theta) \cdot \frac{\pi D_{bore}^2}{4} \left(\frac{d\theta}{dt} \right) \tag{3}$$

$$Q_{pull} = R(\theta) \cdot \frac{\pi \left(D_{bore}^2 - D_{rod}^2 \right)}{4} \left(\frac{d\theta}{dt} \right) \tag{4}$$

$$P_{push} = \frac{T_{CGA}}{R(\theta)} \frac{4}{\pi D_{bore}^2} \tag{5}$$

$$P_{pull} = \frac{T_{CGA}}{R(\theta)} \frac{4}{\pi \left(D_{bore}^2 - D_{rod}^2 \right)} \tag{6}$$

where T_{CGA} is the joint torque from CGA data, $d\theta/dt$ is the calculated derivative of the CGA angle data, and $R(\theta)$ is the actuator moment arm (Fig. 3).

For all required pressures (derived from Eq. 5 and Eq. 6), the valves must be able to provide more than the necessary flow rate (derived from Eq. 3 and Eq. 4). To calculate the maximum flow rate through the valve, Q_V, for any given pressure, a model is set up based on orifice equations [21]:

$$Q_V = \begin{cases} \dfrac{C_D \cdot A_{1,\max}}{\sqrt{\rho}} \sqrt{P_S \left(1 - \dfrac{P}{P_S} \right)} & x_v > 0 \\ -\dfrac{C_D \cdot A_{2,\max}}{\sqrt{\rho}} \sqrt{P_S \left(1 + \dfrac{P}{P_S} \right)} & x_v < 0 \end{cases} \tag{7}$$

where P is the differential pressure in the actuator (P_{push} or P_{pull}), P_S is the supply pressure, C_d is a constant valve coefficient, $A_{i,max}$ are the fully-open valve port cross-sectional areas, x_v is the valve spool position, and ρ is the fluid density. $C_D \cdot A_{1,\max} / \sqrt{\rho}$ and $C_D \cdot A_{2,\max} / \sqrt{\rho}$ are constant for the valve and can be determined either from testing or manufacturer data. The maximum positive and negative flow rates of the BLEEX valves (calculated by Eq. 7) along with the required actuator flow rates (Eq. 3 and Eq. 4) are illustrated in Fig. 9 – Fig. 11. These plots show that for all the required actuator pressures, the

valves can provide larger flow rates than required by the CGA data and selected actuators.

For simplification, the valve equations (Eq. 7) assume that the valves do not leak, the fluid is incompressible, the same flow rate enters and leaves the valve (e.g. the rod area is negligible), and the return pressure is negligible.

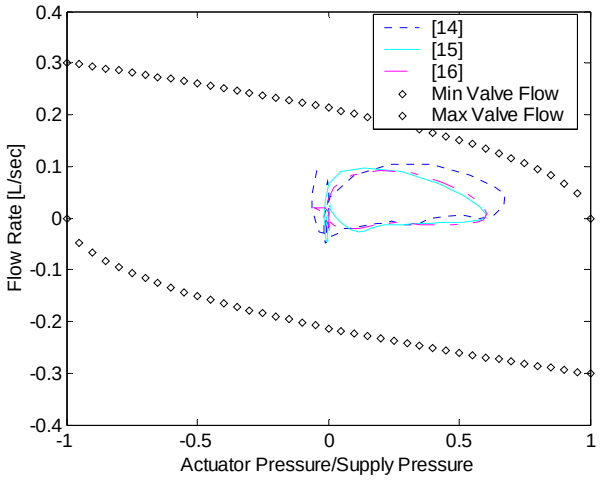

Fig. 9: Ankle Flow Rate vs. Pressure (from CGA data and actuator selection) and Maximum Valve Flow Rates.

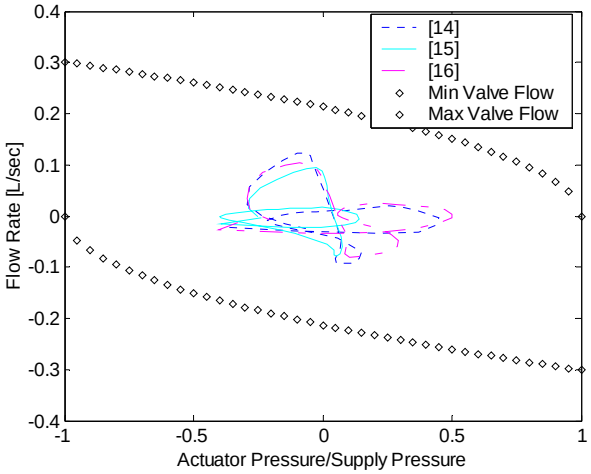

Fig. 10: Knee Flow Rate vs. Pressure (from CGA data and actuator selection) and Maximum Valve Flow Rates.

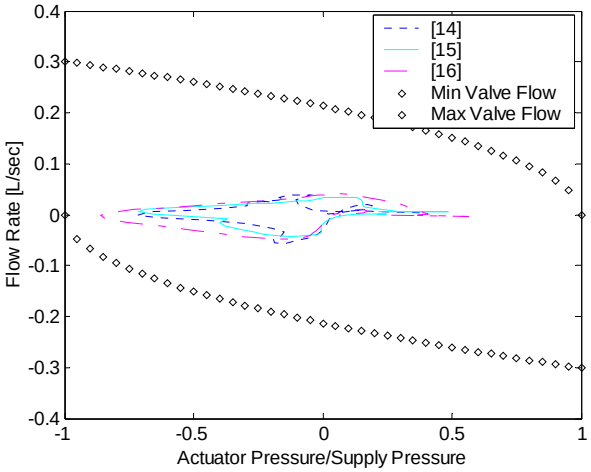

Fig. 11: Hip Flow Rate vs. Pressure (from CGA data and actuator selection) and Maximum Valve Flow Rates.

POWER ANALYSIS

Once the actuators were selected, the required hydraulic power for BLEEX to walk was estimated. Adding the absolute value of the ankle, knee, and hip flow rates for both the right and left legs yields the required system flow rate. Multiplying the system flow rate by the supply pressure (6.9 MPa) results in the total predicted hydraulic power consumption for BLEEX to walk, shown in Fig. 12.

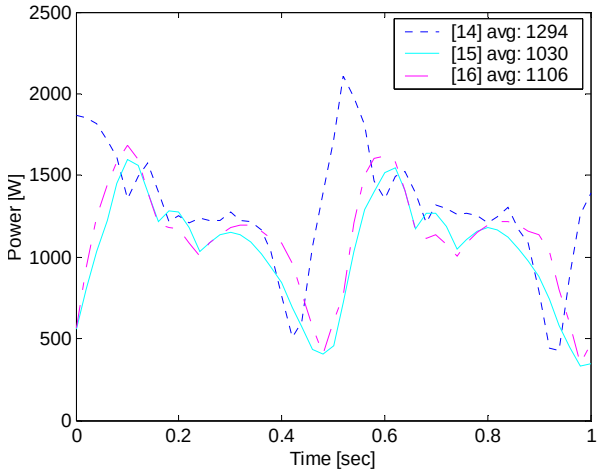

Fig. 12: Hydraulic Power Requirement for BLEEX Walking

The average hydraulic power consumption for BLEEX to walk is 1143 W, compared with 165 W of mechanical power consumed by a human during walking, according to CGA data [19]. The 14% efficiency of the hydraulic actuation is due to the pressure drop across the servo valves when the actuators require less pressure than the supply pressure. Even though it is a fairly low efficiency, this is standard for variable hydraulic systems and when comparing mechanical systems to their biological counterparts. A custom portable power source based on internal combustion engines was developed to create the large amount of power necessary to operate BLEEX [22].

BLEEX DESIGN

Fig. 13 is an overall model of BLEEX (simplified to emphasize the major components). The following sections discuss the critical features of the major components.

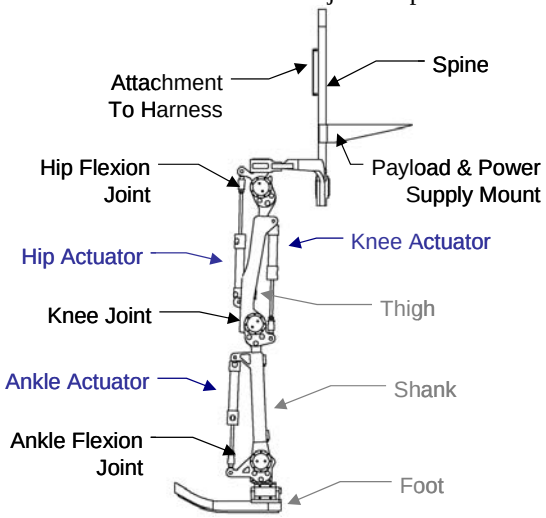

Fig. 13: BLEEX Model (simplified to emphasize major components)

A. Foot Design

The BLEEX foot is a critical component due to its variety of functions:

- It contains the ankle's 3 DoF in a tight space preventing the human foot from feeling constrained.
- It measures the location of the foot's center of pressure and therefore identifies the foot's configuration on the ground. This information is necessary for BLEEX control [12].
- It measures the human's load distribution (how much of the human's weight is on each leg), which is also used in BLEEX control.
- It transfers BLEEX's weight to the ground, so it must have structural integrity and exhibit long life in the presence of periodic environmental forces.
- It is one of two places where the human and exoskeleton are rigidly connected, so it must be comfortable for the operator.

Like the human's ankle, the BLEEX ankle has 3 DoF. The flexion/extension axis coincides with the human ankle joint. For design simplification, the abduction/adduction and rotation axes on the BLEEX ankle do not pass through the human's leg and form a plane outside of the human's foot (Fig. 14). To take load off of the human's ankle, the BLEEX ankle abduction/adduction joint is sprung towards vertical, but the rotation joint is completely free.

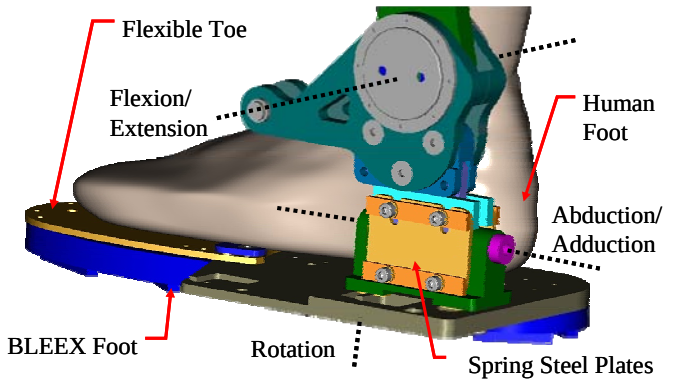

Fig. 14: BLEEX Ankle Degrees of Freedom. Only the flexion/extension axis passes through the human's ankle joint. Abduction/adduction and rotation axes are not powered, but are equipped with appropriate impedances.

Along the bottom of the foot, switches are used to detect which parts of the foot are in contact with the ground. Fig. 15 illustrates the original foot switch concept implemented with digital tape switches in a row along the foot. Each individual switch is labeled as to which of the four "zones" it is in: toe, ball, midsole, or heel. Fig. 16 is a later concept which utilized pressure sensitive rubber between two copper sheets. The rubber changes its resistance as a function of pressure allowing for the switch's on/off threshold to be arbitrarily set. This concept also permits the four zones to be arbitrarily shaped and the soldered wire joints to be eliminated. For robustness, all of the foot sensors were molded into the middle of the foot's rubber sole.

Fig. 15: Original Foot Switches Designed with Digital Tape Switches. Note the four "zones": toe, ball, midsole, and heel.

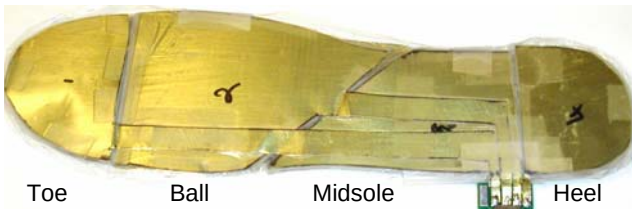

Fig. 16: Foot Switch Concept using Pressure Sensitive Rubber. It allows for arbitrary design of toe, ball, midsole, and heel "zones" and control of the on/off threshold.

As shown in Fig. 17, the main structure of the foot has a stiff heel to transfer the load to the ground and a flexible toe for comfort. The operator's boot rigidly attaches to the top of the exoskeleton foot via a quick release binding. Also illustrated in Fig. 17 is the load distribution sensor, a rubber "pressure tube" filled with hydraulic oil and sandwiched between the human's foot and the main exoskeleton foot structure. Only the weight of the human (not the exoskeleton) is transferred onto the pressure tube and measured by the sensor. This sensor is used by the control algorithm to detect how much weight the human places on their left leg versus their right leg.

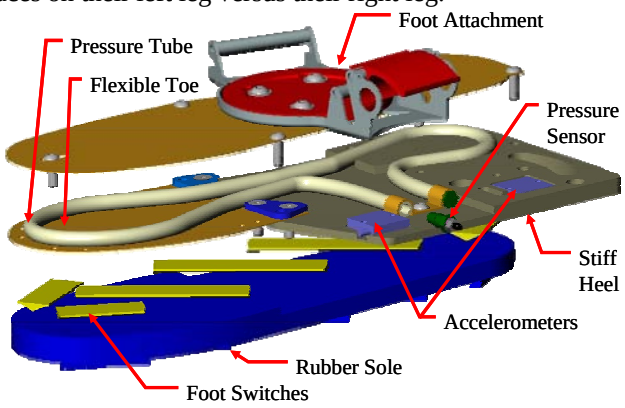

Fig. 17: BLEEX Foot Design (exploded view)

B. Shank and Thigh Design

The main function of the BLEEX shank and thigh are for structural support and to connect the flexion/extension joints together (Fig. 18 and Fig. 19). Both the shank and thigh are designed to adjust to fit 90 percent of the population; they consist of two pieces that slide within each other and then lock at the desired length.

To minimize the hydraulic routing, manifolds were designed to route the fluid between the valves, actuators, supply, and return lines. These manifolds mount directly to the cylinders to reduce the hydraulic distance between the valves and actuator, maximizing the actuator's performance. The actuator, manifold, and valve for the ankle mount to the shank, while the actuators, manifold, and valves for the knee and hip

are on the thigh. One manifold, mounted on the knee actuator, routes the hydraulic fluid for the knee and hip actuators.

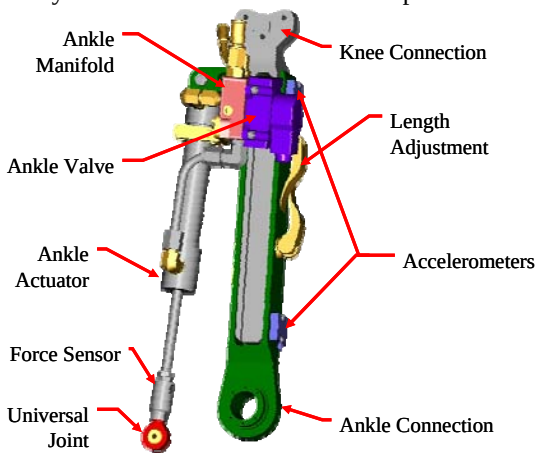

Fig. 18: BLEEX Shank Design

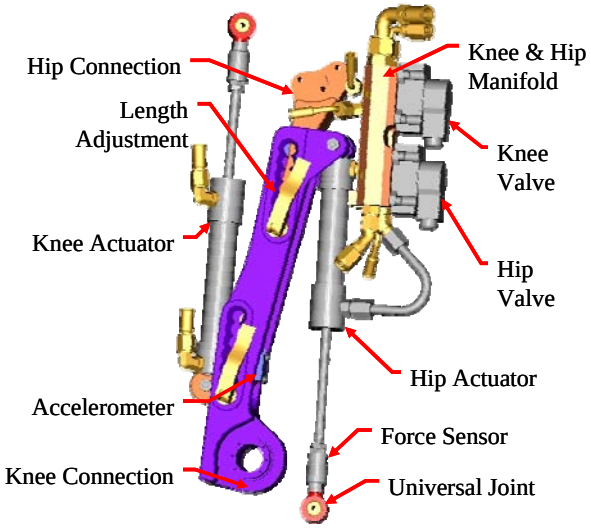

Fig. 19: BLEEX Thigh Design

C. *Hip Design*

It is natural to design a 3 DoF exoskeleton hip joint such that all three axes of rotation pass through the human ball and socket hip joint as seen in the original BLEEX hips in Fig. 20. However, through the design of several mockups and experiments, we learned that these designs have limited ranges of motion and result in singularities at some human hip postures. Therefore the rotation joint was moved so it does not align with the human's hip joint. Initially the rotation joint was placed directly above each exoskeleton leg (labeled "alternate rotation" in Fig. 21). This worked well for the lightweight plastic mockup, but created problems in the full-scale prototype because the high mass of the torso and payload created a large moment about the unactuated rotation joint. Therefore, the current hip rotation joint for both legs was chosen to be a single axis of rotation directly behind the person and under the torso (labeled "current rotation" in Fig. 21). The current rotation joint is typically spring loaded towards its illustrated position using sheets of spring steel.

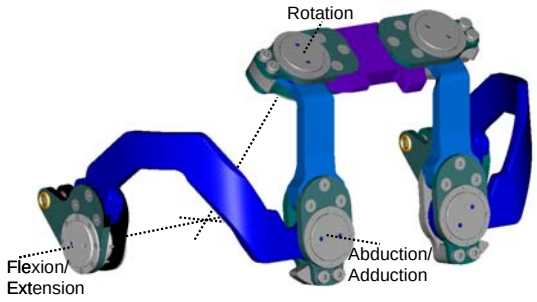

Fig. 20: Original BLEEX Hip Joint (back view). All three of the hip joint axes pass through one point which aligns with the user's ball and socket hip joint.

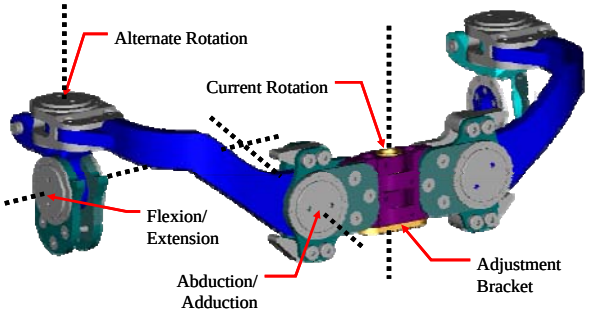

Fig. 21: BLEEX Hip Degrees of Freedom (back view). Only the rotation axis does not pass through the human hip ball and socket joint. The adjustment bracket is replaceable to accommodate various sized operators.

D. *Torso Design*

Shown in Fig. 22, the BLEEX torso connects to the hip structure (shown in Fig. 21). The power supply, controlling computer, and payload mount to the rear side of the torso. An inclinometer mounted to the torso gives the absolute angle reference for the control algorithm. A custom harness mounts to the front of the torso to hold the exoskeleton to the operator. Besides the feet, the harness is the only other location where the user and exoskeleton are rigidly connected. Fig. 22 also illustrates the actuator, valve, and manifold for the hip abduction/adduction joint.

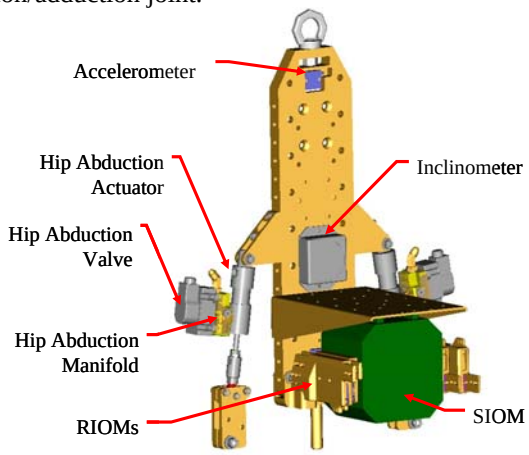

Fig. 22: BLEEX Torso Design (back view)

Custom electronic boards (called remote I/O modules or RIOMs) are used to acquire all of the sensor data and communicate with the control computer (called the supervisor I/O module or SIOM) [13]. Some of the RIOMs along with the SIOM are attached to the BLEEX torso and illustrated in Fig. 22. The other RIOMs are attached to the shanks and thighs, but were omitted from the figures for clarity.

E. Final Design

Fig. 23 shows the current BLEEX design. The black backpack encloses the power source, controller computer, and payload.

Fig. 23: Final BLEEX Design

EXPERIMENTALLY MEASURED PERFORMANCE

The exoskeleton actuation was designed using human CGA data, which assumes that the BLEEX kinematics and dynamics closely match human leg kinematics and dynamics. To verify this assumption, and for use in future exoskeleton development, torque and angle data was measured from BLEEX walking. The measured data for the ankle, knee, and hip flexion/extension joints are shown in Fig. 24 – Fig. 26. The figures show both the torque desired by the controller, and the torque actually measured from the sensors. Additionally, the plots show the actuator limit curves so the measured data can be easily compared with the CGA curves (Fig. 5 – Fig. 7).

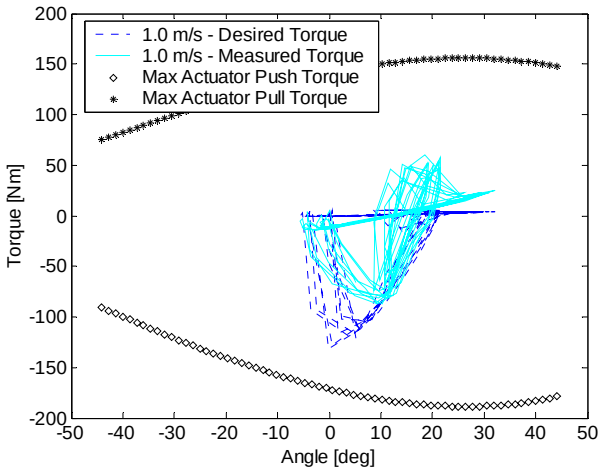

Fig. 24: Ankle Torque vs. Angle Data Measured from BLEEX Walking

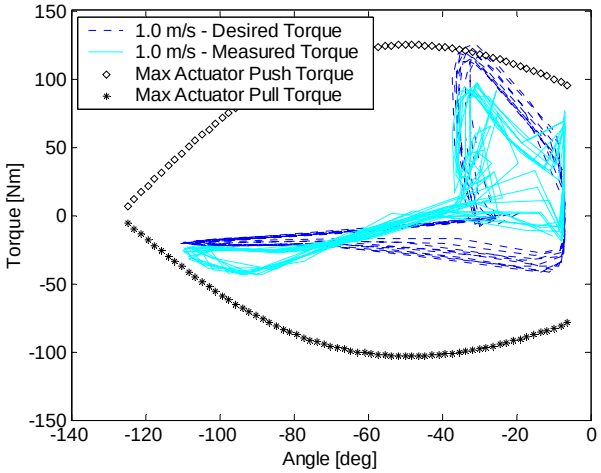

Fig. 25: Knee Torque vs. Angle Data Measured from BLEEX Walking

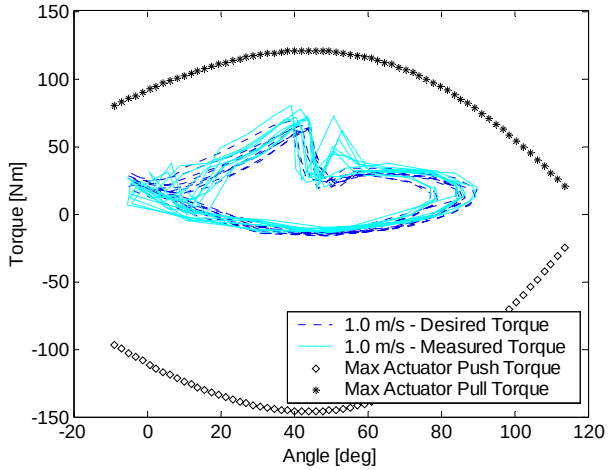

Fig. 26: Hip Torque vs. Angle Data Measured from BLEEX Walking

All of the measured torque curves lie within the maximum actuator curves, which shows BLEEX has sufficient torque to walk without saturating the actuators. However, a quick comparison of the measured torque vs. angle curves (Fig. 24 – Fig. 26) and CGA torque vs. angle curves (Fig. 5 – Fig. 7) reveals that there are some distinct differences. Some of the more significant causes for these discrepancies are listed below:

- The BLEEX knee is always bent by at least 5° allowing the leg to always exert a vertical force. This offsets the ankle and hip angles slightly positive and the knee angle slightly negative. The bent knee also shifts the required knee torques more positive than a straight knee.
- While the BLEEX torso weighs close to a human torso, its center of gravity is behind the human torso's center of gravity. This creates a negative shift of the ankle and hip torques and a positive shift in the knee torque.
- The local torque control on each joint actuator is not perfected, so the desired torques are not always achieved.

Generally, measured data from the knee and hip joints differ the most from the CGA data used to design the actuation. Both the knee and hip also consume more energy per step (area encircled by a torque/angle curve) than predicted, but the ankle consumes less energy.

ACKNOWLEDGEMENTS

The work is partially funded by DARPA grant DAAD19-01-1-509.

CONCLUSIONS AND FUTURE WORK

Approximating the BLEEX kinematics and dynamics as the same as human leg kinematics and dynamics allowed the BLEEX actuation to be designed based on CGA data. This resulted in a BLEEX leg with 7 DoF and four of them are actuated (flexion/extension at the ankle, knee, and hip and abduction/adduction at the hip). The actuator sizes, actuator mounting points, and servo valves were also selected utilizing CGA data. Initial calculations indicated that BLEEX should consume about 1140 W of power while walking. The measured torque vs. angle curves from BLEEX demonstrate that the CGA-based design yielded an exoskeleton with sufficient torque to walk. However, the measured curves do differ from the CGA curves, showing that the BLEEX kinematics and dynamics do not fully match the human, so further design improvement can be accomplished based around the more accurate, measured torque vs. angle curves.

While there is still significant work remaining, BLEEX has successfully walked while carrying its own weight and producing its own power. This makes BLEEX the first energetically autonomous lower extremity exoskeleton capable of carrying a payload. Currently BLEEX has been demonstrated to support up to 75 kg (exoskeleton weight + payload), walk at speeds up to 1.3 m/s, and shadow the operator through numerous maneuvers without any human sensing or pre-programmed motions.

Current work on BLEEX includes continued analysis of the measured performance data in order to improve the actuation design and efficiency. Considerable work is also being performed to decrease the overall power consumption of BLEEX, either by reduced actuation, additional passive elements, or improved efficiency. Hopefully with continued improvement to the system's fieldability, the BLEEX will become a practical method of increasing human carrying capacity and endurance through rough environments.

REFERENCES

[1] Makinson, B.J., General Electric Co., 1971, "Research and Development Prototype for Machine Augmentation of Human Strength and Endurance, Hardiman I Project", *Technical Report S-71-1056*, Schenectady, NY.

[2] Vukobratovic, M., Hristic, D., and Stojiljkovic, Z., Jan. 1974, "Development of Active Anthropomorphic Exoskeletons." *Medical and Biological Engineering*, pp. 66-80.

[3] Kawamoto, H. and Sankai, Y., 2002, "Power Assist System HAL-3 for Gait Disorder Person." Lecture Notes in Computer Science, **2398**, *Proceedings of the Eighth International Con. on Computers Helping People with Special Needs*, Berlin, Germany.

[4] Yamamoto, K., Hyodo, K., Ishii, M., and Matsuo, T., Sept. 2002, "Development of Power Assisting Suit for Assisting Nurse Labor." *JSME International Journal Series C.*, **45(3)**.

[5] Mori, Y., Takayama, K., and Nakamura, T., May 2004, "Development of Straight Style Transfer Equipment for Lower Limbs Disabled." *Proceedings of the IEEE International Conference on Robotics and Automation*, **3**, New Orleans, Louisiana, pp. 2486-2491.

[6] Johnson, D., Repperger, D., and Thompson, G., Mar. 1996, "Development of a Mobility Assist for the Paralyzed, Amputee, and Spastic Patient." *Proceedings of the Fifteenth Southern Biomedical Engineering Conference*, IEEE, Dayton, Ohio, pp. 67-70.

[7] Misuraca, J. and Mavroidis, C., Nov. 2001, "Lower Limb Human Muscle Enhancer." *Proceedings of the Symposium on Advances in Robot Dynamics and Control, ASME International Mechanical Engineering Congress and Exposition*, New York, New York.

[8] Pratt, J., Krupp, B., Morse, C., and Collins, S., May 2004, "The RoboKnee : An Exoskeleton for Enhancing Strength and Endurance during Walking." *Proceedings of the IEEE Int. Conference on Robotics and Automation (ICRA)*, **3**, New Orleans, Louisiana, pp. 2430-2435.

[9] Fleischer, C., Reinicke, C., and Hommel, G., Aug. 2005, "Predicting the Intended Motion with EMG-Signals for an Exoskeleton Orthosis Controller." *Proceedings of IEEE International Conference on Intelligent Robots and Systems*, Edmonton, Canada, in press.

[10] Naruse, K., Kawai, S., Yokoi, H., and Kakazu, Y., Nov. 2003, "Design of Compact and Lightweight Wearable Power Assist Device." *Proceedings of ASME International Mechanical Engineering Congress and Exposition*, Washington D.C.

[11] Ferris, D., Czerniecki, J., and Hannaford, B., Aug. 2001, "An Ankle-Foot Orthosis Powered by Artificial Muscles." *Proceedings of the 25th Meeting of the American Society of Biomechanics*, San Diego, California.

[12] Kazerooni, H., Huang, L., and Steger, R., April 2005, "On the Control of the Berkeley Lower Extremity Exoskeleton (BLEEX)", *IEEE International Conference on Robotics and Automation*, Barcelona, Spain.

[13] Kim, S., Anwar, G., and Kazerooni, H., June 2004, "High-Speed Communication Network for Controls with Application on the Exoskeleton", *American Control Conference*, Boston.

[14] Winter, A., International Society of Biomechanics, Biomechanical Data Resources, Gait Data. Available: http://www.isbweb.org/data/

[15] Kirtley, C., "CGA Normative Gait Database", Hong Kong Polytechnic University. Available: http://guardian.curtin.edu.au/cga/data/

[16] Linskell, J., CGA Normative Gait Database, Limb Fitting Centre, Dundee, Scotland. Available: http://guardian.curtin.edu.au/cga/data/

[17] Woodson, W., Tillman, B., and, Tillman, P., 1992, "Human Factors Design Handbook", New York: McGraw-Hill, pp. 550-552.

[18] Rose, J. and Gamble, J.G., 1994, *Human Walking*, Second Edition, Williams & Wilkins, Baltimore.

[19] Chu, A., Kazerooni, H., and, Zoss, A., April 2005, "On the Biomimetic Design of the Berkeley Lower Extremity Exoskeleton (BLEEX)", *IEEE International Conference on Robotics and Automation*, Barcelona, Spain.

[20] Riener, R., Rabuffetti, M., and, Frigo, C., 2002, "Stair Ascent and Descent at Different Inclinations", *Gait and Posture*, **15**, pp. 32-34.

[21] Fox, R., McDonald, A., 1998, *Introduction to Fluid Mechanics*, John Wiley and Sons, New York, New York.

[22] Amundson, K., Raade, J., Harding, N., and, Kazerooni, H., Aug. 2005, "Hybrid Hydraulic-Electric Power Unit for Field and Service Robots", *IEEE International Conference on Intelligent Robots and Systems*, Edmonton, Canada, in press.

